Optimal Temperature Control for Batch Beer Fermentation

Douglas A. Gee and W. Fred Ramirez
Department of Chemical Engineering, University of Colorado, Boulder, Colorado 80309

Accepted for publication February 10, 1987

Optimal control theory was applied to the process of batch beer fermentation. The performance functional considered was a weighted sum of maximum ethanol production and minimum time. Calculations were based on the model of Engasser et al. modified to include temperature effects. Model parameters were determined from isothermal batch fermentations. The fermentor cooling duty was the single available control. Temperature state variable constraints as well as control variable constraints were considered. The optimal control law is shown to be bang-bang control with the existence of a singular arc corresponding to isothermal operation at the maximum temperature constraint. An iterative algorithm is presented for computing appropriate switching times using a penalty-function-augmented performance functional.

INTRODUCTION

It is common in industrial beer fermentations to operate at an experimentally determined optimal growth temperature for the yeast being used. Depending on how the fermentation progresses, the temperature can be raised (i.e., to speed up a slow fermentation) or lowered (i.e., to offset the formation of undesirable flavor and aroma compounds) to keep the fermentation on schedule and to maintain the desired product quality. Ideally the temperature should not have to be varied in this way, but unforseen circumstances often arise that require temperature variation.

In this article a simplistic model of beer fermentation is used to perform an optimal temperature control study of beer fermentation. Several good reviews of optimal and nonoptimal control studies of biological processes have been published within the last few years.[1-3] Among the work that has been done are various studies of the temperature control of biological processes including beer fermentation,[4-6] although to our knowledge no applications of optimal control theory to the control of beer fermentation temperature have been done.

MATHEMATICAL MODEL

The mathematical model of beer fermentation used was based on the work of Engasser.[7] The Engasser model was modified for this work by including temperature effects in the kinetic rate expressions and by adding temperature as a state variable.

The fermenting medium was assumed to contain three sugars, glucose, maltose, and maltotriose, as the limiting nutrients. The rates of uptake of the three sugars are given by the equations:

Glucose:

$$\frac{dG}{dt} = -\mu_1(G)X \tag{1}$$

Maltose:

$$\frac{dM}{dt} = -\mu_2(M,G)X \tag{2}$$

Maltotriose:

$$\frac{dN}{dt} = -\mu_3(N,M,G)X \tag{3}$$

where:

$$\mu_1(G) = \frac{V_G G}{K_G + G} \tag{4}$$

$$\mu_2(M,G) = \frac{V_M M}{K_M + M}\frac{K'_G}{K'_G + G} \tag{5}$$

$$\mu_3(N,M,G) = \frac{V_N N}{K_N + N}\frac{K'_G}{K'_G + G}\frac{K'_M}{K'_M + M} \tag{6}$$

and

G = glucose concentration, mol/m^3
M = maltose concentration, mol/m^3
N = maltotriose concentration, mol/m^3
X = biomass concentration, mol/m^3
μ_i = specific rate of sugar uptake, h^{-1}
V_i = maximum reaction velocity for ith sugar ($i = G$, M, or N), h^{-1}
K_i = Michaelis constant for ith sugar ($i = G, M,$ or N), mol/m^3
K'_i = inhibition constant for ith sugar ($i = G$ or M)

The rates of biomass and ethanol production were proportionally related to the uptakes of the individual sugars by

Biotechnology and Bioengineering, Vol. 31, Pp. 224–234 (1988)

CCC 0006-3592/88/030224-11$04.00

constant yield coefficients. The resulting expressions were then integrated directly to give the following algebraic equations for the ethanol and biomass concentrations (note that $E(t_0) = 0$):

$$X(t) = X(t_0) + R_{X_G}[G(t_0) - G(t)] + R_{X_M}[M(t_0) - M(t)] + R_{X_N}[N(t_0) - N(t)] \quad (7)$$

$$E(t) = R_{E_G}[G(t_0) - G(t)] + R_{E_M}[M(t_0) - M(t)] + R_{E_N}[N(t_0) - N(t)] \quad (8)$$

where

R_{X_i} = stoichiometric yield of biomass per mole of sugar reacted, $i = G$, M, or N, assumed constant

R_{E_i} = stoichiometric yield of ethanol per mole of sugar reacted, $i = G$, M, or N, assumed constant

Yeast flocculation has not been well characterized, and although Engasser et al. observed that flocculation depended on the glucose concentration for their yeast,[7] this was not observed for our yeast, which remained in suspension until late in the fermentation, long after glucose had disappeared from the medium. Therefore, for simplicity, the biomass concentration described by Eq. (7) was considered to consist of the sum of the suspended and flocculated yeast in the vessel (i.e., the total yeast present in the fermentor). This was deemed sufficient for the purpose of ethanol production optimization investigated here. However, a more comprehensive model including flavor and aroma compound concentrations as well as yeast flocculation would be needed for a more extensive optimal control study such as one in which an optimal flavor profile is sought.

The rate of temperature change in the fermenting medium was given by

$$\frac{dT}{dt} = \frac{1}{\rho C_p}\left[\Delta H_{F_G}\frac{dG}{dt} + \Delta H_{F_M}\frac{dM}{dt} + \Delta H_{F_N}\frac{dN}{dt} - u(T - T_c)\right] \quad (9)$$

With

$$u = \frac{UA}{V} \quad (10)$$

and

C_p = mixture heat capacity (assumed constant), kJ/kg °C

ρ = mixture density (assumed constant), kg/m^3

T = temperature, °C

ΔH_{F_i} = heat of reaction, ($i = G$, M, or MT, assumed constant), kJ/mol

u = control variable (fermentor cooling rate), kJ/h m^3 °C

U = overall heat transfer coefficient (assumed constant), kJ/h m^2 °C

A = heat transfer area, m^2

V = volume of fermenting mixture, m^3

T_c = coolant temperature, °C

In Eq. (9) it was assumed that heat of mixing effects due to carbon dioxide evolution during the fermentation were negligible.

Van Uden[8] has noted that the kinetic rate constants in biological reactions of yeast follow an Arrhenius-type temperature dependence up to a defined optimal growth temperature. Most researchers, as a first approximation, have assumed a temperature dependence only on the maximum specific rate parameters and have ignored any similar effects on other kinetic parameters. In fitting the model to data it was found that these parameters did vary with temperature and that they followed an Arrhenius dependency quite closely (see Figs. 4–6). Based on this, the maximum rate velocities, Michaelis constants, and inhibition constants in Eqs. (4)–(6) are parameterized (for $i = G$, M, or MT) as

$$V_i = V_{i0}\exp[-E_{V_i}/R(T + 273.15)] \quad (11)$$

$$K_i = k_{i0}\exp[-E_{K_i}/R(T + 273.15)] \quad (12)$$

$$K_i' = k_{i0}'\exp[-E_{K_i'}/R(T + 273.15)] \quad (13)$$

where

V_{i0} = Arrhenius frequency factor for maximum velocity, h^{-1}

k_{i0} = Arrhenius frequency factor for Michaelis constant, mol/m^3

k_{i0}' = Arrhenius frequency factor for inhibition constant, mol/m^3

E_{V_i} = Arrhenius activation energy for maximum velocity, cal/mol

E_{K_i} = Arrhenius activation energy for Michaelis constant, cal/mol

$E_{K_i'}$ = Arrhenius activation energy for inhibition constant, cal/mol

R = gas constant, 1.987 cal/mol °K

The Engasser model also included the formation of various flavor and aroma compounds. However, their production was modeled as proportional to the yeast growth rate so that no control of their formation could ever be obtained using this model. Once a yeast growth profile was determined, the flavor and aroma profiles would be fixed according to the model. It is for this reason that these compounds were not included in this model even though they are important factors in beer fermentation. This shortcoming of the Engasser model demonstrates the need for a new and more comprehensive mathematical model of beer fermentation.

MODEL PARAMETER DETERMINATION

Values for the stoichiometric yields of ethanol and biomass were obtained from Harrison and Graham's balanced overall reaction for production of ethanol and biomass from glucose by yeast[9]:

$$C_6H_{12}O_6 + 0.224C_4H_6O_2N \rightarrow 1.97CO_2 + 1.92C_2H_6O \quad (14)$$

(glucose) (amino acids) (ethanol)

$$+ 0.04C_3H_8O_3 + 0.008C_4H_6O_4 + 0.134CH_{1.67}O_{0.5}N_{0.17} + 0.011H_2O$$

(secondary metabolites) (biomass)

The heats of reaction were also calculated based on values given by Williams.[9] The values found for the stoichiometric yields (R_{E_i}, R_{X_i}) and the heats of fermentation (ΔH_{F_i}) are shown in Table I.

Table I. Reaction parameters.

Sugar	$R_{E/i}$	$R_{X/i}$	ΔH_{R_i} kJ/mol
Glucose	1.92	0.134	− 91.2
Maltose	3.84	0.268	−226.3
Maltotriose	5.76	0.402	−361.3

EXPERIMENTAL

Four isothermal batch fermentations were run simultaneously in 100-L nonagitated conical fermentors to determine the model kinetic parameters. A typical brewery yeast strain (*S. carlsbergensis*) and a typical brewery wort were used in the fermentations. The original gravity of the wort was 16 degrees Plato (weight percent sugar), and it was aerated before fermentation to a dissolved oxygen concentration of 7 ppm. Yeast counts were done on all four fermentations only at the start to give the initial yeast concentrations required by the model. Transient sugar concentration data were obtained at 4, 8, 12, and 16°C. These temperatures effectively cover the range considered feasible for beer fermentations. Concentrations of glucose, maltose, and maltotriose were determined by HPLC. The specific gravity of the beer was measured at all sampling times.

DATA REGRESSION

The model was fitted to the data using the following algorithm: (1) Initial model parameter values were guessed and fed by a driver routine to the IMSL nonlinear regression subroutine ZXSSQ.[10] (2) ZXSSQ then used a Levenberg–Marquardt algorithm to minimize the sum of squares of the residual errors with respect to a set of model parameters. This routine was called by the driver program and it, in turn, called subroutine MODEL. (3) Subroutine MODEL integrated the model equations over the entire fermentation time using the parameter values supplied by ZXSSQ and computed the residual errors between the data and model. These were then fed back to ZXSSQ. (4) ZXSSQ then computed the partials of the sum of squares with respect to the parameters and used these partials to determine new parameter values. (5) Steps 3 and 4 were repeated until the change in the sum of squares from one iteration to the next fell below a given tolerance. Fitting the data proved to be a difficult task because multiple local optima were encountered in the fitting process. Accurate results were dependent on good initial starting conditions.

Figure 1 shows the comparison between data and the model fit at each experimental temperature. As seen from this figure, the sugar concentration data were a bit irregular. Much of this was due to the sampling technique used, wherein samples were taken during fermentation and frozen for later analysis. Since the yeast was not removed before

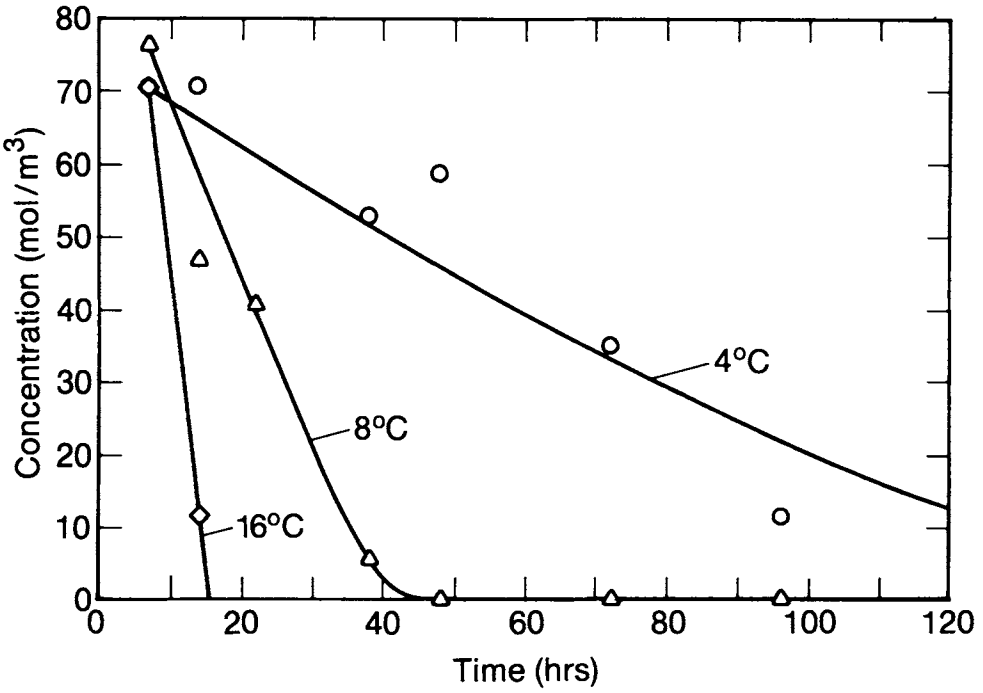

Figure 1. Model fit for glucose at different temperatures. Lines give model fit, symbols are data points (+ , 16°C; △, 8°C; × , 4°C).

freezing, the samples were found to have continued fermenting to various degrees upon thawing for analysis. This effect is shown most dramatically in Fig. 3, where the samples that continued fermenting as they thawed can easily be identified. The irregular data shown in Fig. 3 are not representative of all the data taken but were included here to demonstrate the problems encountered with the sampling methods used. Most of the data were regular enough to allow a reliable model parameter fit to be performed (Figs. 1 and 2). The final kinetic parameters are given in Table II.

Figure 1 shows the need for the Monod-type expression to describe the uptake of sugars by yeast. At 16° the uptake of glucose exhibits definite zero-order behavior. As the fermentation temperature decreases, the behavior of glucose

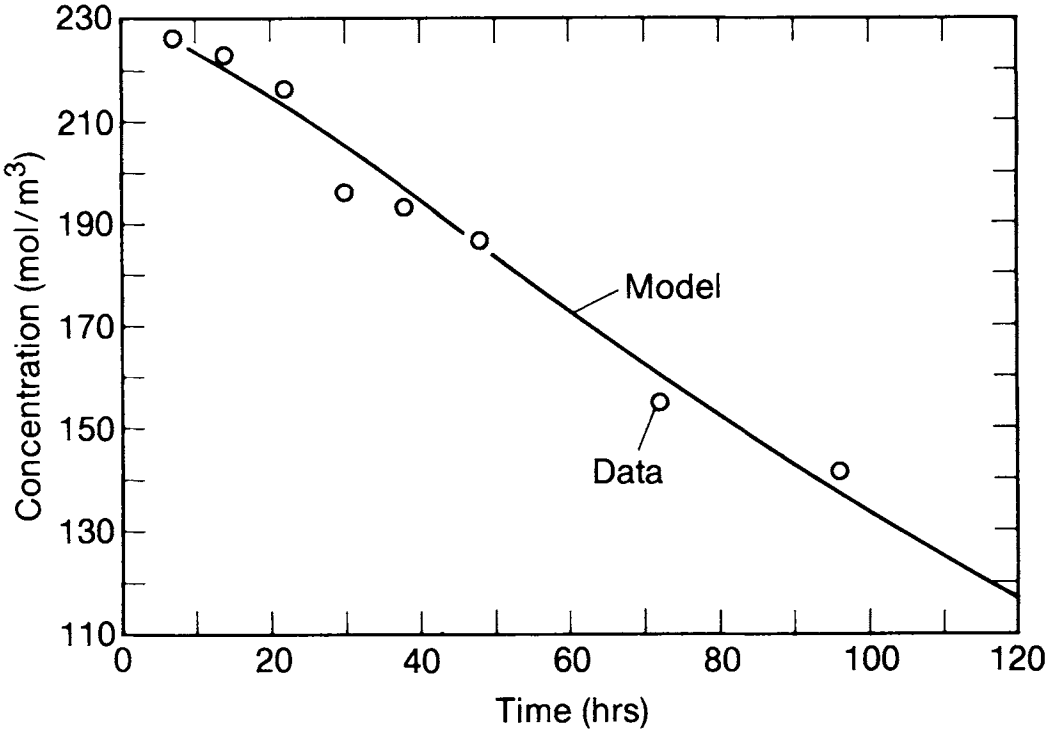

Figure 2. Model fit for maltotriose at 4°C: line, model fit; +, data.

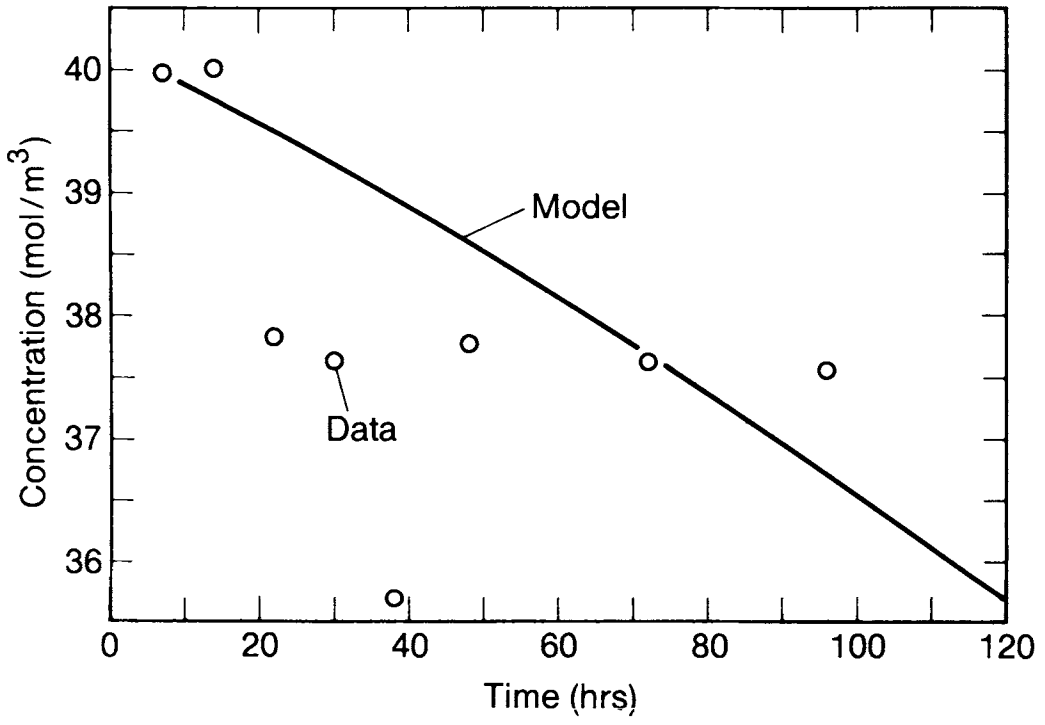

Figure 3. Model fit for maltose at 8°C: line, model fit; +, data.

Table II. Kinetic parameters.

Parameter	Fermentation temperature			
	4°C	8°C	12°C	16°C
V_G (h^{-1})	0.0048	0.013	0.015	0.0302
V_m (h^{-1})	0.0144	0.0268	0.028	0.0364
V_N (h^{-1})	0.087	0.113	0.13	0.151
K_G (mol/m^3)	23.5	4.7	1.8	0.102
K_M (mol/m^3)	1,100	814	610	360
K_N (mol/m^3)	10,900	7,160	4,460	2,410
K'_G (mol/m^3)	123	182	240	262
K'_M (mol/m^3)	2,090	6,360	8,010	17,500

becomes logarithmic in nature as evidenced by the 4° curve. The Monod expression is shown here to be capable of describing this phenomenon accurately.

As seen in Table II, the maximum velocity constants for each sugar show an increase with increased temperature while the Michaelis constants for each sugar decrease with increasing temperature. The net effect is, therefore, for the rate of sugar consumption to increase with temperature under all conditions, as expected. Similarly, the data showed inhibition effects to be more important at low temperatures than at high temperatures. This implies that the inhibition constants K'_G and K'_M should increase with temperature as was found here.

The rate constants of Table II were used to compute the Arrhenius constants for each model parameter. This was done by performing a linear least-squares fit to an Arrhenius plot for each parameter. The Arrhenius constants found for each of the model parameters are shown in Table III. Typical Arrhenius plots and the straight-line fits for each parameter are shown in Figs. 4–6.

Table III. Arrhenius constants.

Parameter	Activation energy (kcal/mol)	Natural Logarithm of frequency factor
V_G	22.6	35.77
V_M	11.3	16.40
V_N	7.16	10.59
K_G	−68.6	−121.3
K_M	−14.4	− 19.15
K_N	−19.9	− 26.78
K'_G	10.2	23.33
K'_M	26.3	55.61

CONTROL THEORY

For this model of beer fermentation, it was desired to obtain a maximum final ethanol concentration within a minimum batch time. Therefore, the objective functional to be minimized is

$$J = -E(t_f) + w\int_0^{t_f} dt \tag{15}$$

where w is a weighting factor. Expressing the model equations in state variable form gives

$$\dot{x} = f(x, \dot{x}, u, t) \tag{16}$$

where

$$x_1 = G \qquad x_2 = M \qquad x_3 = N \qquad x_4 = T \tag{17}$$

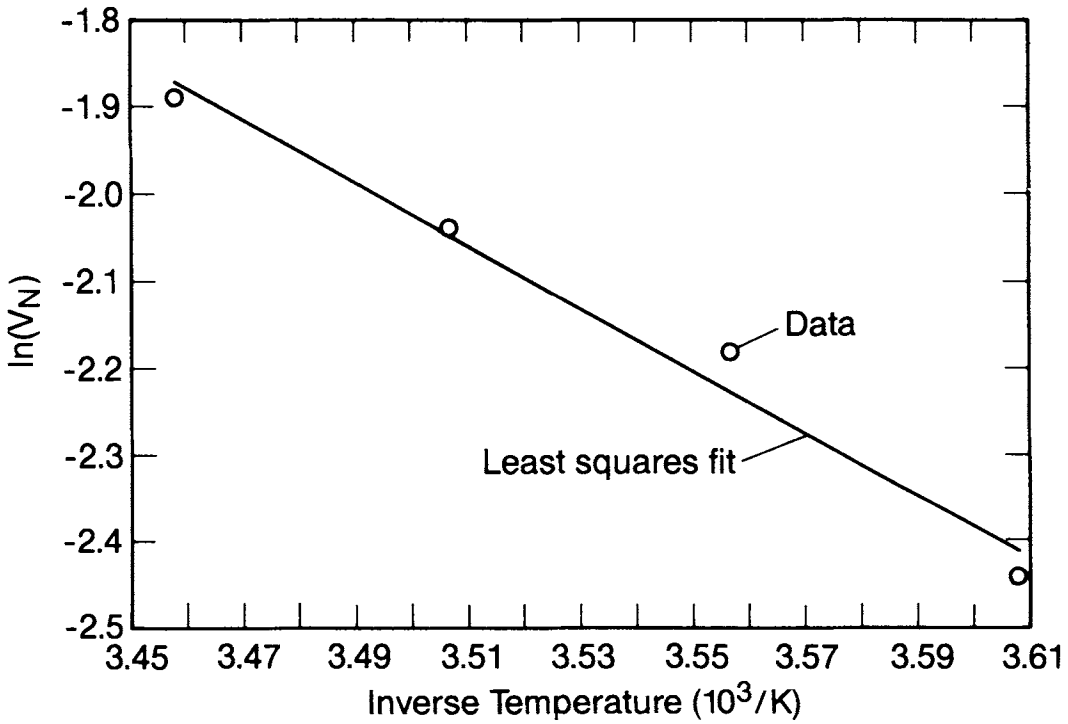

Figure 4. Arrhenius plot for V_N: line, linear least-squares fit; □, data.

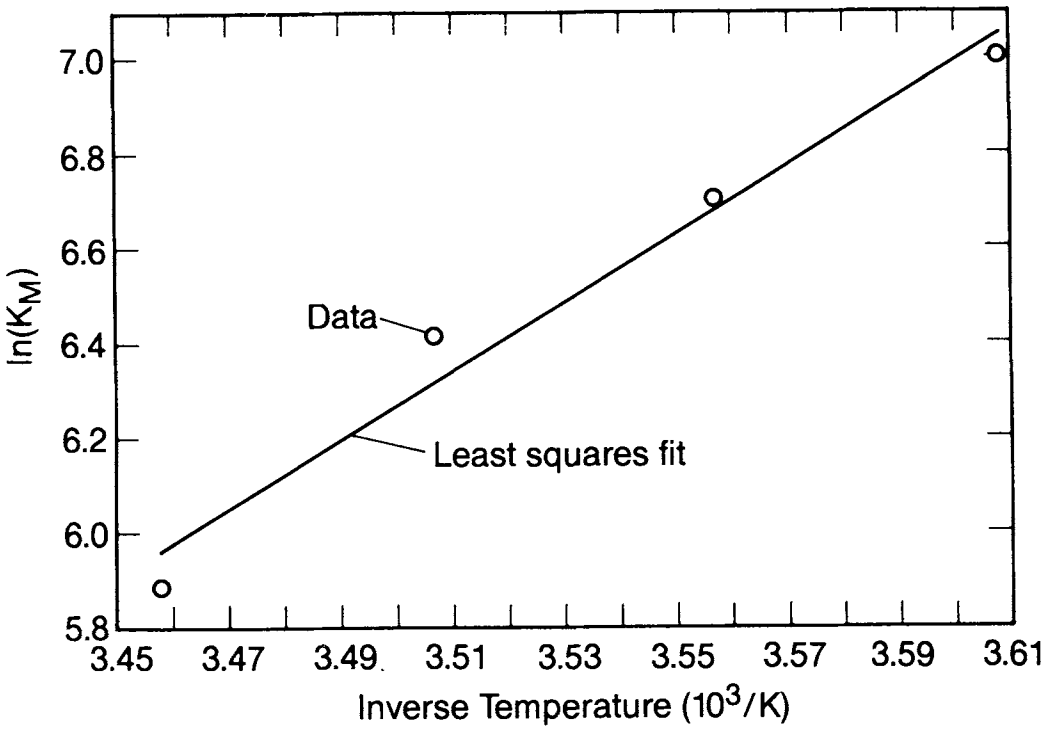

Figure 5. Arrhenius plot for K_M: line, linear least-squares fit; □, data.

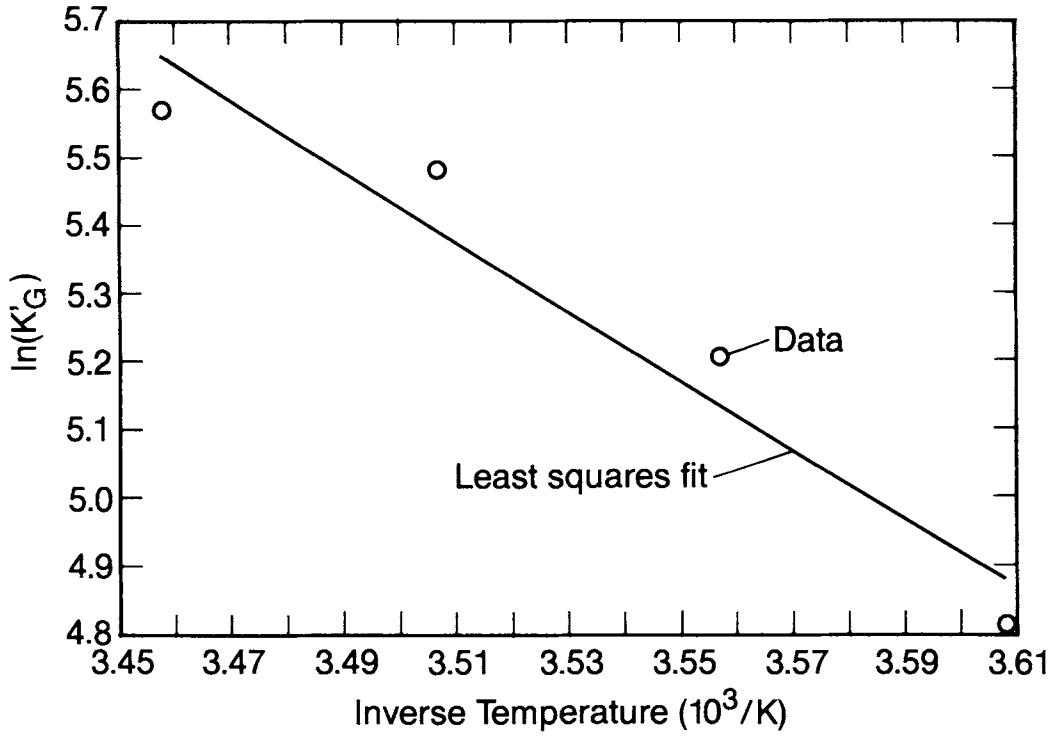

Figure 6. Arrhenius plot for K'_G: line, linear least-squares fit; □, data.

The objective functional becomes

$$J = \sum_{i=1}^{3} R_{E_i}[x_i(t_f) - x_i(0)] + w\int_0^{t_f} dt \qquad (18)$$

It was also desired to constrain the control and the temperature within physically realistic values. The constraints imposed were

$$0°C \leq T \leq T_{max} \qquad (19)$$

and

$$u_{min} \leq u \leq u_{max} \qquad (20)$$

Condition (19) was satisfied by letting $T_c = 0$°C in the state Eq. (9) and by adding a penalty function in the objective functional to satisfy the maximum temperature constraint. Optimization with constraints on the control variable requires applying Pontryagin's minimum principle.[11]

An augmented performance index is formed (including the penalty function) as

$$J' = \sum_{i=1}^{3} R_{E_i}[x_i(t_f) - x_i(t_0)] - \int_0^{t_f} L\,dt \tag{21}$$

where L is the Lagrangian defined by

$$\mathrm{L} = w + \lambda^T(f - \dot{x}) + Q(x_4 - T_{\max})^2 U(x_4 - T_{\max}) \tag{22}$$

$U(x_4 - T_{\max})$ is the unit step function defined by

$$U(x_4 - T_{\max}) = \begin{cases} 0 & \text{if } x_4 < T_{\max} \\ 1 & \text{if } x_4 \geq T_{\max} \end{cases} \tag{23}$$

and Q is a large positive weighting value

From variational calculus[11] the necessary conditions for a minimum can be derived for this system as follows:

1. Costate equations:

$$\dot{\lambda}_1 = \frac{\Delta H_{F_1}}{\rho C_p}\dot{\lambda}_4 - \sum_{i=1}^{3} \lambda_i \frac{\delta f_i}{\delta x_1} \tag{24}$$

$$\dot{\lambda}_2 = \frac{\Delta H_{F_2}}{\rho C_p}\dot{\lambda}_4 - \sum_{i=1}^{3} \lambda_i \frac{\delta f_i}{\delta x_2} \tag{25}$$

$$\dot{\lambda}_3 = \frac{\Delta H_{F_3}}{\rho C_p}\dot{\lambda}_4 - \sum_{i=1}^{3} \lambda_i \frac{\delta f_i}{\delta x_3} \tag{26}$$

$$\dot{\lambda}_4 = -\sum_{i=1}^{4} \lambda_i \frac{\delta f_i}{\delta x_4} - 2Q(x_4 - T_{\max})U(x_4 - T_{\max}) + Q(x_4 - T_{\max})^2\,\delta(x_4 - T_{\max}) \tag{27}$$

where δ is the Dirac delta function.

2. State equations:

$$\dot{x} = f(x, \dot{x}, u) \tag{28}$$

3. Boundary conditions: In this case $x(0)$ is known. By transversality,

$$\lambda_1(t_f) = R_{E_1} \tag{29}$$

$$\lambda_2(t_f) = R_{E_2} \tag{30}$$

$$\lambda_3(t_f) = R_{E_3} \tag{31}$$

$$\lambda_4(t_f) = 0 \tag{32}$$

The final time is given by the condition

$$H(t_f) = 0 \tag{33}$$

where the Hamiltonian is defined as

$$H = L - \dot{x}^T \frac{\partial L}{\partial x} \tag{34}$$

4. Optimal control: By Pontryagin's maximum principle, we have

$$\text{If } \lambda_4 > 0 \quad \text{then } u = u_{\max} \tag{35}$$

$$\text{If } \lambda_4 < 0 \quad \text{then } u = u_{\min} \tag{36}$$

and

$$\text{If } \lambda_4 = 0 \text{ and stays zero,} \quad \text{then } u = u_{\text{singular}} \tag{37}$$

The intermediate control law of Eq. (37) implies, using Eq. (27), that x_4 must equal $T_{\max}$ for singular control. Along such an isothermal path, we must have $\partial f_i/\partial x_4 = 0$ since $\lambda_i \neq 0$. Due to the penalty function constraint, such an isothermal path is reached at the constraint temperature $T_{\max}$. From the temperature state Eq. (9), we can compute the singular control to be

$$u_{\text{singular}} = \frac{1}{(T_{\max} - T_c)\rho C_p} \times [\Delta H_{F_2}\dot{x}_1 + \Delta H_{F_2}\dot{x}_2 + \Delta H_{F_3}\dot{x}_3] \tag{38}$$

The following algorithm was used to find the optimal control for this problem: (1) A constant control was assumed at $u = u_{\max}$. (2) The state equations were integrated forward in time until the final time was reached as indicated by Eq. (33). (3) The costate equations were integrated backward in time from the final to the initial time, and the controller was calculated at each time based on the fourth costate variable. When the penalty function effect was detected ($x_4 > T_{\max}$), the singular control policy of Eq. (38) was implemented, and λ_4 was set to zero. Along the singular arc it is possible that the control constraint could be violated. In that case the control variable is set to $u_{\max}$. (4) The control policy found in step 3 was then used in integrating the states as in step 2. (5) Steps 3 and 4 were repeated until the routine converged to a specific optimal control.

APPLICATIONS

Figures 7–10 show the constrained optimal temperature operation for a 100-L fermentor. Table IV gives the equipment parameters and starting wort conditions used in this example. The control policy is to let $u = u_{\min}$ (minimum cooling) until the maximum allowable temperature is attained. At this point the singular control policy is initiated as shown in Figs. 9 and 10.

In some cases the maximum amount of cooling required for operating along the singular arc might not be available. This is illustrated by the following example, which is the same problem described in Table IV except that the maximum cooling capacity was lowered to 30 KJ/m^3 h °C. The optimal controller is shown in Fig. 10 for comparison with the unconstrained controller. It started out at $u_{\min}$, and the temperature increased until a specific time indicated by the switching of the fourth costate variable was reached. At this time the controller switched to operation at $u_{\max}$ to slow the rate of reaction. Operation continued at $u_{\max}$ with the temperature slowly rising to an intersection with $T_{\max}$ as shown in Fig. 9. At this point the controller switched to the singular arc of isothermal operation at $T_{\max}$ until the final time was

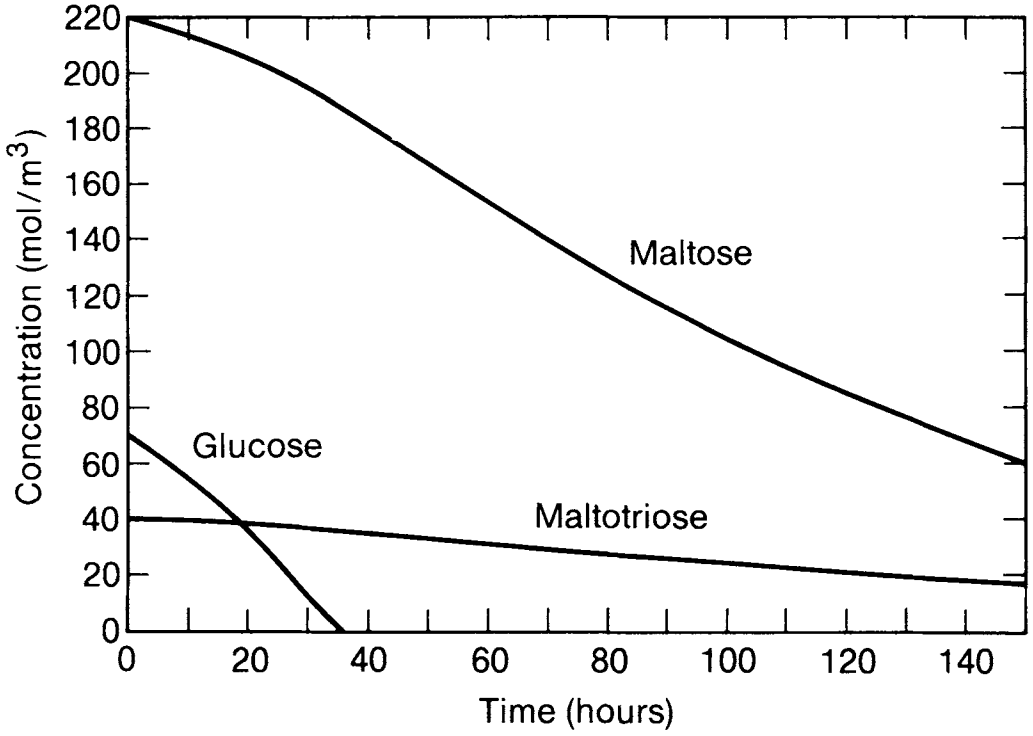

Figure 7. Simulation of optimal fermentation sugar profile: △, glucose; × , maltose; ▽, maltotriose.

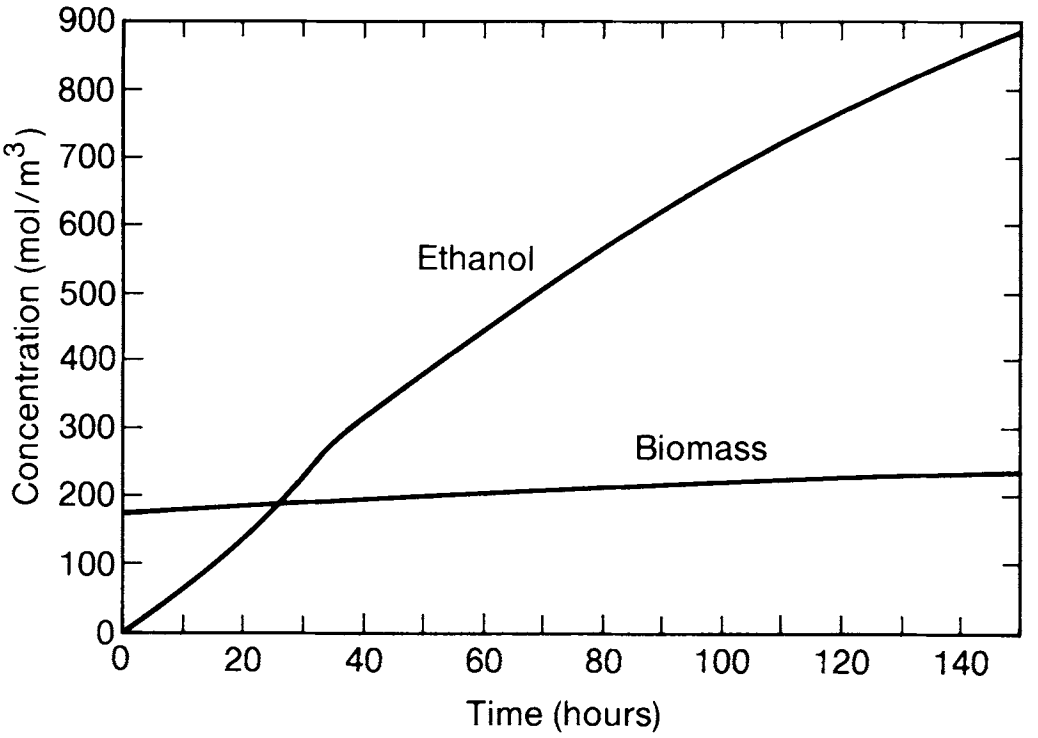

Figure 8. Simulation of optimal fermentation ethanol and biomass profiles: ◇, biomass; △, ethanol (×0.2).

achieved. This optimal control policy allowed the fermentor to operate at the maximum possible temperature at all times without violating the maximum refrigeration constraint.

Finding the switching times in this example required implementation of optimal control theory as it was not obvious *a priori* what these times should have been. The action of

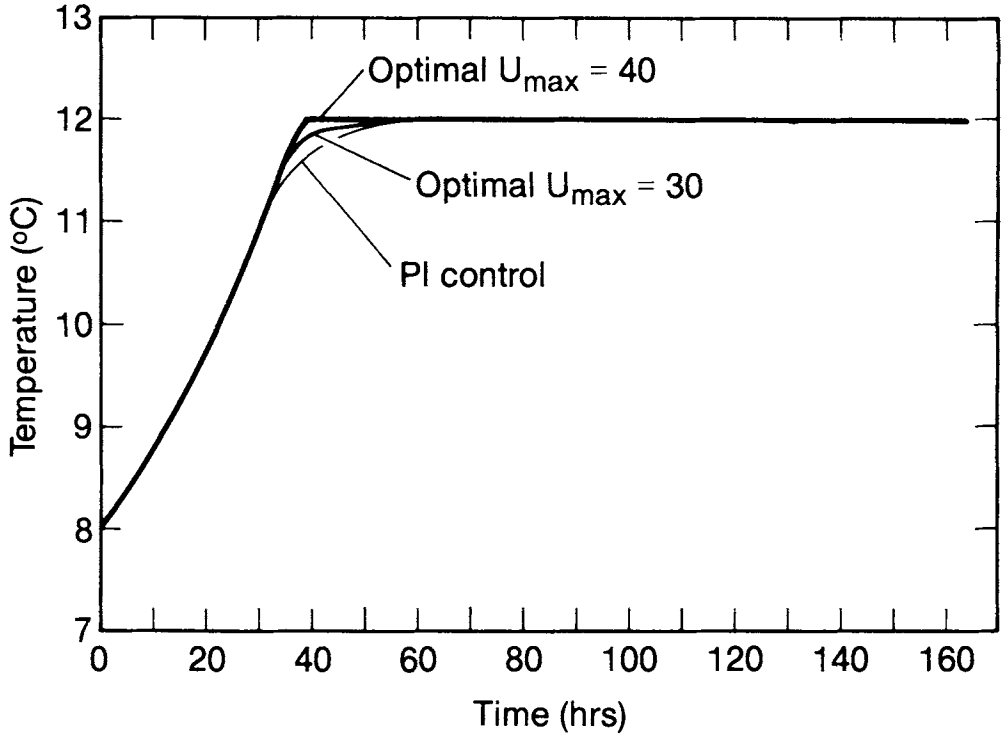

Figure 9. Temperature profiles for three cases: ◇, simulation of optimal profile with u_{max} = 40; △, simulation of optimal profile with u_{max} = 30; ▽, simulation of PI control temperature profile.

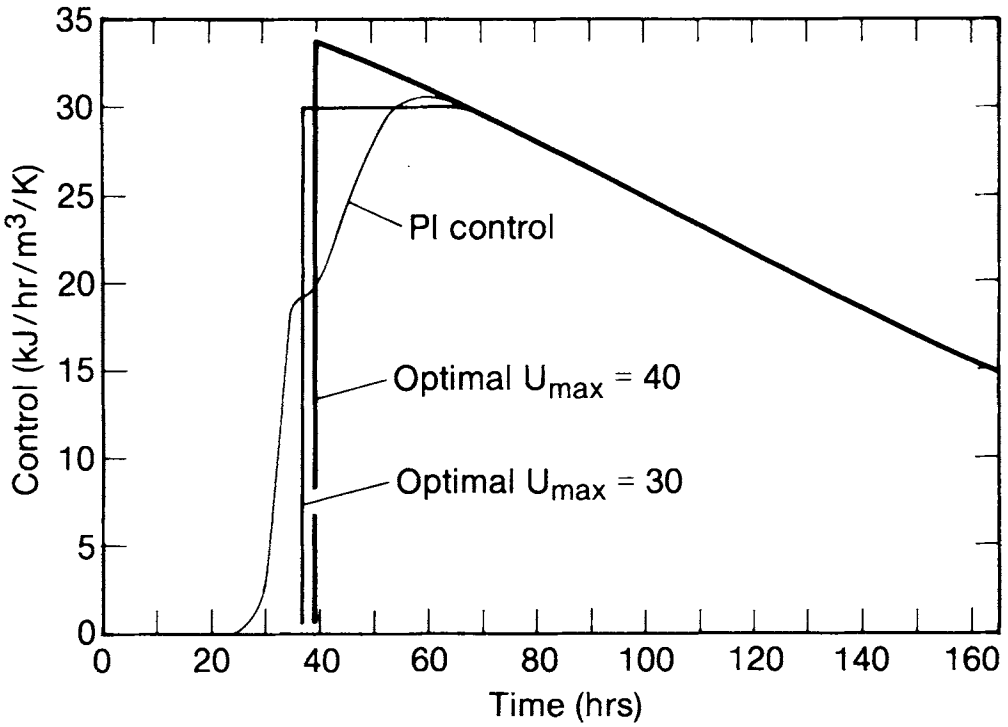

Figure 10. Controller profiles for three cases: ◇, simulation of optimal profile with u_{max} = 40; △, simulation of optimal profile with u_{max} = 30; + , simulation of PI control profile.

the fourth costate variable in iteratively computing the controller is the only clear way to find these optimal switching points.

The weighting factor w is the most important variable affecting the final product of the optimal fermentation. Typical values of $E(t_f)$ are on the order of 10^3, while the final time

Table IV. Initial conditions and equipment parameters.

$G(t_0) = 70$ mol/m^3	$X(t_0) = 125$ mol/m^3
$M(t_0) = 220$ mol/m^3	$T(t_0) = 8$°C
$N(t_0) = 40$ mol/m^3	
$A = 0.188$ m^2	$u_{min} = 0$ J/m^3 h °C
$C_p = 4016$ J/kg °C	$u_{max} = 4 \times 10^4$ J/m^3 h °C
$\rho = 1040$ K g/m^3	V = 0.1 m^3

is usually on the order of 10^2 in magnitude. Therefore, for small values of w (i.e., $w = 0$ to $w = 1$), the effect of ethanol in the objective functional is considerably more important than that of the final time. Therefore, for these weightings the computed optimal control results in high final ethanol concentrations and long batch times. For $w = 0.1$, the fermentation proceeds essentially to completion with practically no minimum time influence at all. At a w of 1 the fermentation produces 96% of the ethanol in about two-thirds the time required for $w = 0.1$. Table V gives computed values of $E(t_f)$, t_f, and the objective functional for various values of w. As can be seen in the table, if w gets large enough, the final time portion of the objective functional can become so important as to give the optimal fermentation as being no operation at all (e.g., $w = 8$). Therefore, the choice of the weighting factor must be made based on the relative importance of the batch time and the desired final ethanol concentration for the individual process application. All simulations described in this article were performed using a weighting factor of 3.

A conventional PI controller was used to control a simulation of the process for comparison with the optimal controller. A maximum temperature of 12°C was used as the setpoint for the PI controller. Both the optimal controller and the PI controller were simulated using an initial temperature of 8°C. The PI controller was tightly tuned in order to allow the fastest possible response time with zero overshoot to avoid violating the maximum temperature constraint (critically damped case). Figure 9 shows the temperature as a function of time for the optimal and PI controllers. The PI simulation was run the same amount of time as the optimal simulation for comparison. Although the PI controller performed admirably, it still resulted in a larger value of the objective functional than the optimal controller ($J' = -430$ for the PI vs. $J' = -433$ for the optimal controller). However, the PI controller approached the optimal controller so closely that, judging from the ease of implementation, it would make sense industrially to implement the PI rather than the optimal controller with a slight loss of performance. The PI controller is shown in Figure 10 for comparison with the two optimal controllers.

Table V. Effect of weighting factor w on optimal fermentation.

w	$E(t_f)$ ($\times 10^{-3}$ mol/m^3)	t_f (h)	J' ($\times 10^{-2}$)
0.1	1.20	314	−11.7
0.5	1.18	236	−10.7
1.0	1.16	203	−9.58
2.0	1.11	171	−7.73
5.0	0.957	123	−3.40
6.0	0.895	112	−2.22
7.0	0.287	36.1	−0.346
8.0	0	0	0

The main insight gained by this study was that, based on this simple model, it was found that the isothermal temperature operating policies that have often been used in beer fermentation are actually optimal singular arc policies for maximizing alcohol concentration in minimum time. A bang-bang policy should be used to optimally approach the singular arc. The simplicity of the model used in generating these results must not be overlooked. The model neglected some potentially important effects such as ethanol inhibition effects and temperature effects on the flavor and aroma components in the product. Considering the latter effect, it is very possible that at certain points during beer fermentation, the process can be accelerated by raising the temperature without changing the final product, while raising the temperature during other phases of the process might change the flavor and aroma characteristics of the final product drastically. This, in fact, has been observed.[5] These are the effects that will have the greatest influence on an implementable optimal temperature control policy for beer fermentation, and they do not even appear in this model.

It should also be noted that temperature control is not the only option open for the control of beer fermentation. A more complex model might include controllable effects such as addition of various nutrients or oxygen at certain times during the process in order to facilitate an acceleration of the process. These types of control may actually prove more promising than any elaborate temperature control policy.

CONCLUSIONS

Based on this simple model, the optimal controller to yield a maximum final ethanol concentration in the minimum time is to allow the temperature to attain its maximum possible value at all times during the fermentation. The optimal cooling control is a combination of bang-bang and isothermal arc policies. Switching times must be computed via optimal control theory for each specific application.

The study showed that one of the current temperature control policies used industrially is actually the singular arc of optimal operation. However, since the model did not include the effects of temperature on flavor and aroma components, it is possible that a more elaborate temperature control policy would actually be optimal to obtain desired flavor and aroma characteristics in the final product. Therefore, a more comprehensive model of beer fermentation is needed that includes these effects before a true optimal control policy for beer fermentation can be determined.

NOMENCLATURE

A	heat transfer area (m^2)
C_p	mixture heat capacity (kJ/kg °C)
E	ethanol concentration (mol/m^3)

E_{K_i} Arrhenius activation energy for Michaelis constants, $i = G, M,$ or N (cal/mol)
$E_{K_i'}$ Arrhenius activation energy for inhibition constants, $i = G$ or M (cal/mol)
E_{V_i} Arrhenius activation energy for maximum reaction velocities, $i = G, M,$ or N (cal/mol)
f_i derivatives of state variables (x_i)
G glucose concentration (mol/m^3)
H Hamiltonian
ΔH_{F_i} heats of reaction for sugars (kJ/mol)
J objective functional
J' objective functional augmented by state equations and penalty function
K_i Michaelis constant for ith sugar (mol/m^3)
K_i' inhibition constant for ith sugar (mol/m^3)
K_{i0} Arrhenius frequency factor for ith Michaelis constant (mol/m^3)
K_{i0}' Arrhenius frequency factor for ith inhibition constant (mol/m^3)
L Lagrangian
λ costate variables
M maltose concentration (mol/m^3)
N maltotriose concentration (mol/m^3)
Q weighting factor
R gas constant, 1.987 cal/mol K
R_{E_i} molar yield of ethanol per mole of ith sugar reacted
R_{X_i} molar yield of biomass per mole of ith sugar reacted
ρ mixture density (kg/m^3)
t time (h)
t_f final time (h)
t_0 initial time (0.0 h)
T fermentation temperature (°C)
T_c coolant temperature (°C)
u control variable, cooling rate (J/h m^3 °C)
u_{max} maximum allowable controller setting (J/h m^3 °C)
u_{min} minimum allowable controller setting (J/h m^3 °C)
U overall heat transfer coefficient (J/h m^2 °C)
V mixture volume (m^3)
V_i maximum reaction rate for ith sugar (h^{-1})
V_{i0} Arrhenius frequency factor for maximum velocity constant of ith sugar (h^{-1})
w weighting factor
X biomass (yeast) concentration (mol/m^3)
x_1 represented G in optimal control model formulation (mol/m^3)
x_2 represented M in optimal control model formulation (mol/m^3)
x_3 represented N in optimal control model formulation (mol/m^3)
x_4 represented T in optimal control model formulation (°C)

References

1. N. S. Wang and G. Stephanopoulos, *CRC Crit. Rev. Biotechnol.*, **2**(1), 1 (1985).
2. P. Agrawal and H. C. Lim, in *Advances in Biochemical Engineering/Biotechnology,* Vol. 30, A. Fiechter, Ed. (Springer-Verlag, New York, 1984), p. 61.
3. S. J. Parulekar and H. C. Lim, in *Advances in Biochemical Engineering/Biotechnology,* Vol. 32, A. Fiechter, Ed. (Springer-Verlag, New York, 1985), p. 207.
4. W. R. Haas, L. L. Tavlarides, and W. J. Wnek, *AIChE J.*, **20**(4), 707 (1974).
5. H. Miedaner, *The Brewer,* February 1978, p. 33.
6. A. Sadana, *AIChE J.*, **25**(3), 535 (1979).
7. J. M. Engasser, I. Marc, M. Moll, and B. Duteurtre, EBC Congress 1981, p. 579.
8. N. Van Uden, in *The Yeasts,* Vol. 2, A. H. Rose and J. S. Harrison, Eds. (Academic, London, 1971), p. 91.
9. L. A. Williams, *Am. J. Enol. Viticult.*, **33**(3), 149 (1982).
10. IMSL Software Library, Nonlinear Regression Routine ZXSSQ.
11. D. E. Kirk, *Optimal Control Theory: An Introduction* (Prentice-Hall, Englewood Cliffs, NJ, 1970), p. 228.